Phase evolution of terahertz radiation from femtosecond laser-induced air plasma

ZHEN ZHANG,[1] YANPING CHEN,[1,2,*] ZHELIN ZHANG, [1,2,4] TIANHAO XIA,[1,2]
JIAYANG ZHANG,[1,2] ZHENGMING SHENG,[1,2,3,4] AND JIE ZHANG[1,2]

[1] *Key Laboratory for Laser Plasma (Ministry of Education), School of Physics and Astronomy, Shanghai Jiao Tong University, Shanghai 200240, China*
[2] *IFSA Collaborative Innovation Center, Shanghai Jiao Tong University, Shanghai 200240, China*
[3]*Department of Physics, SUPA, University of Strathclyde, Glasgow G4 0NG, UK*
[4]*Tsung-Dao Lee Institute, Shanghai, China.*
**Corresponding author: yanping.chen@sjtu.edu.cn*

The phase evolution of terahertz radiation from single-color femotsecond laser induced air plasma controlled by a DC-bias is investigated experimentally. When the DC-bias is moved from the end to the beginning of the laser-plasma filament, the produced terahertz waveform is advanced temporally and its carrier-envelope phase changed. Our phase spectrum analysis suggests that the slope and the intercept of the phase spectrum determine respectively the temporal shift and the carrier-envelope phase of the terahertz waveform. Therefore, the observed terahertz waveform evolution is mainly due to the THz propagation effect in plasma filament and the Gouy phase shift associated with the detection scheme. Our work also illustrates explicitly the temporal order of terahertz radiation from different parts of a filament.

Femtosecond laser-induced air plasma can radiate terahertz (THz) pulses with high field strength [1] and broad spectral bandwidth [2]. THz waves with high electric fields can be used to study charge carrier dynamics in semiconductors [3], transient photoconductivity in GaAs [4] and impact ionization dynamics[5]. THz spectrum with large bandwidth is beneficial for THz wave remote sensing and spectroscopy [6]. Compared with the terahertz radiation from a laser-irradiated solid target, THz wave generation in air plasma can be driven by intense femtosecond laser pulses with moderate peak power and focused intensity operating at kHz high repetition rates [7]. As the THz pulses produced in this way are usually with few cycles, understanding their phase evolution under different experimental conditions is beneficial for their applications.

A lot of research work has been carried out on the subject of THz waveform evolution. Kim *et al*. showed the change of the temporal THz waveform by controlling the relative phase between fundamental and second harmonic pulses [8]. Bai *et al.* derived the evolution of THz waveforms driven by few-cycle laser pulses from the shift of the carrier phase and the change of the laser envelope during propagation [9]. Zhao *et al*. investigated the propagation effect of THz waves inside the filaments, which is responsible for the significant advancement of the maximum value of the THz waveform generated by the femtosecond laser filament in the air [10]. In the study of THz wave generation by two-color lasers in nitrogen molecules from the supersonic gas nozzle, Li *et al.* revealed that the shift of the waveform was due to the change in the refractive index of the THz wave [11]. In 2018, Li *et al.* confirmed that the competition effect of laser plasma absorption and oscillation currents could determine the evolution of the THz pulses [12]. Zhang *et al.* proposed that the carrier-envelope phase of the THz pulse could be controlled by varying the filament length and the initial phase difference between the two-color laser components [13]. Wang *et al*. have reported that the THz waveform could have a phase shift of π due to the change of the plasma density distribution at the beginning and end of a laser filament [14].

As one's understanding of the evolution of the THz waveform becomes deeper, it is gradually recognized that THz radiation is a superposition of THz waves radiated from different positions of the filament. Panov *et al*. reported the role of constructive interference in the determination of far-field THz profile [15]. You *et al.* demonstrated that the far-field THz radiation profiles are due to off-axis constructive interference between locally generated THz waves along the filament [16]. Zhang *et al.* proposed a radiation model, which suggested that THz radiation from a filament was due to coherently superposition of THz pulses from a linear array of dipoles along the filament [17]. As such, the THz waveform or carrier-envelope phase is closely associated with the temporal order of THz waves radiated from different parts of a long filament, which is still not all clear.

In this Letter, the waveform evolution of THz radiation from a single-color air filament is investigated by changing the position of a slice-shaped external electric field (DC-biased field) applied on the filament. A temporal shift, as well as a change in carrier-envelope phase of the measured THz waveform, can be explained by phase spectral modification due to the THz pulse propagation effect. Our finding is helpful for understanding the physical mechanisms of THz wave generation from femtosecond laser-induced air plasma.

The experimental setup is shown in Fig. 1, where a 1 kHz, 40 fs, 800 nm, 5 mJ laser pulse is focused by a convex lens with a focal length of 30 cm, forming a centimeter-long filament in air. A slice-shaped external DC electric field of 8 kV/cm, induced by two pieces of 3-mm-wide copper strips, was applied perpendicularly on the filament. The copper strips were placed on a motive stage so that it can be translated along the filament. Since the amplitude of the THz pulse from 8 kV/cm DC-biased plasma is about two orders of magnitude higher than that from single-color plasma [18], the measured THz signal in our setup is mainly contributed by THz radiation from plasma zone which is affected by the DC-bias. By scanning the slice-shaped external electric field, THz waves from different parts (DC-biased) of the filament can be collected by two off-axis parabolic mirrors and measured by the electro-optic sampling (EOS) method. We didn't shift the EO crystal while the DC-bias was moved. We optimized the position of the EO crystal when the slice-shaped DC-bias was fixed at z=6mm. The diameter of the off-axis parabolic mirror is 2 inches, and the focal length of the two off-axis parabolic mirrors is about 100 mm. The EO crystal is oriented in $\langle 110 \rangle$, and the thickness of the crystal is about 1.5 mm. The optical

axis of the EO crystal is parallel to the direction of the DC-biased field.

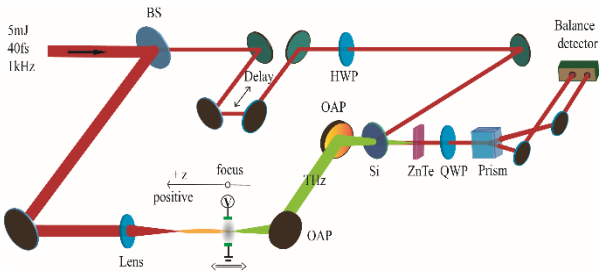

Fig. 1. (Color online) Schematic diagram of the experimental setup. The distance between the center of the slice-shaped DC-bias and the geometric focus of the lens (or the end of the filament) is defined as *z*. BS: beam splitter; OAP: off-axis parabolic; HWP: half-wave plate; QWP: quarter-wave plate.

We measured the waveforms of the THz radiation from DC-biased air filament when the slice-shaped DC-bias was scanned from 0 mm to 15 mm from the geometric focus of the lens (*z*=0 mm to *z*=15 mm), as shown in Fig. 2(a).

One can see that the THz waveform changes slightly as *z* increases. The THz waveforms shown in Fig. 2(a) are not normalized. And the THz amplitude remains substantially unchanged as the electrode moves. Meanwhile, it shows that the peak of the THz waveform advances temporally. Figure 2(b) shows the spectra of the THz waves from Fig. 2(a) at several typical locations. We can find that the peak frequency and bandwidth of the THz wave remain almost unchanged. In order to explore the physical mechanism of this phenomena, we introduce the phase spectrum analysis of THz radiation.

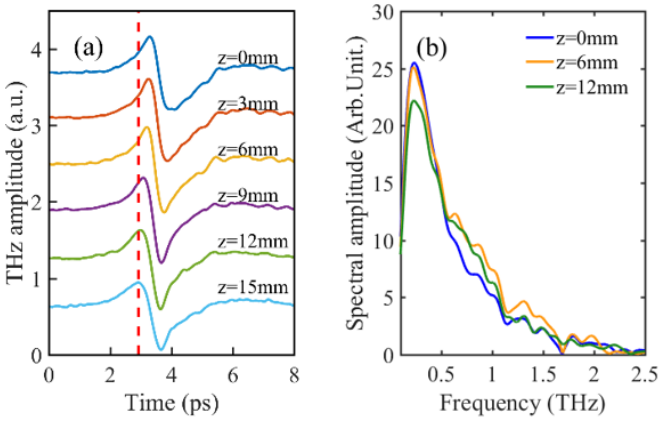

Fig. 2. (a) Measured waveforms of the THz radiation when the slice-shaped DC-bias located at *z*=0, 3, 6, 9, 12 and 15mm. The pump laser energy is 5 mJ. A red dash line is added to help identify the shift of the peak of the waveform. (b) Typical spectra of the THz waveforms at three positions of the DC-biased field.

For a given THz waveform, we can obtain both its amplitude spectrum and phase information using Fourier Transform method, as shown in Fig. 3. Figures 3(a) and 3(c) show typical THz waveforms when slice-shaped DC-biased field is applied respectively at the end and the beginning of the filament, while Figs. 3(b) and 3(d) are their corresponding Fourier transformed spectra (blue curve) and phases (black curve), respectively. It is found that the phase φ has an almost linear relationship with the THz frequency, so it can be expressed by

$$\varphi = \alpha \cdot \Omega + \beta , \quad \textbf{(1)}$$

where α and β are the slope and the intercept of the phase spectrum, Ω is the angular frequency of the THz waves, as shown in Figs. 3(b) and 3(d) (red dashed lines). When the slice-shaped DC-biased field is applied at the end of the filament (z = 0 mm), we have the fitted values $\alpha = -3.56$ ps and $\beta = 0.33\,\pi$ for the THz phase spectra. Here, $\alpha = -3.56$ ps means that a probe pulse arrives 3.56 ps ahead of the THz pulse when measuring the waveform of this THz pulse by the electro-optic sampling method. When the slice-shaped DC-biased field is applied at the beginning of the filament (z =15 mm), we have α=-3.46 ps and $\beta = 0.58\,\pi$. When the THz waveform is different, the phase spectra are different. When the difference between the amplitude spectrum of the THz wave is small, the temporal waveform of the THz wave is mainly determined by the slope and intercept of the phase spectrum. Therefore, we can understand the evolution of the THz waveform by analyzing the changes in the phase spectrum.

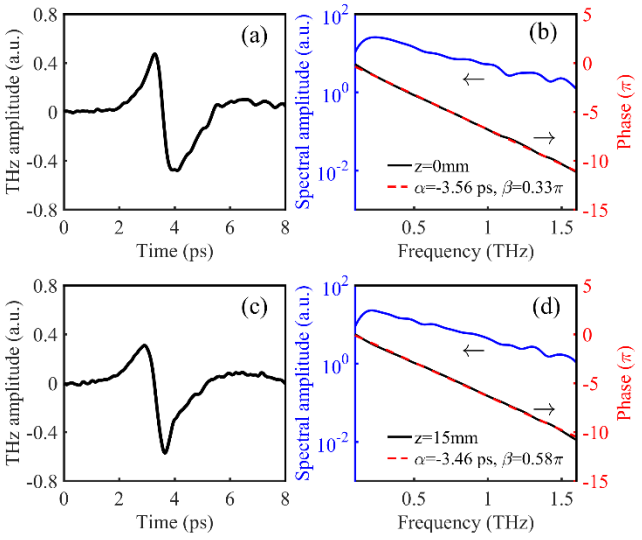

Fig. 3. (a) and (c) show THz waveforms when the DC-bias is applied at z = 0 mm and z = 15 mm. The blue curves in (b) and (d) are the spectra, and black curves in (d) and (d) are the phases. The red dashed line in (b) and (d) are the fitted curves of the phase spectrum, respectively.

In the following, we will clarify the relation between the phase spectra and the corresponding THz waveforms. Assume we have the time domain signal $x(t)$ and its corresponding complex amplitude $X(\Omega)$ in the frequency domain. The relation between $x(t)$ and $X(\Omega)$ satisfies [19]:

$$x(t) = \frac{1}{2\pi}\int_{-\infty}^{\infty} X(\Omega) e^{i\Omega t} d\Omega , \quad \textbf{(2)}$$

In the frequency domain, as the phase changes by $\Delta\varphi = \Delta\alpha \cdot \Omega + \Delta\beta$, the new signal in the time domain $x_n(t)$ can be written as:

$$x_n(t) = \frac{1}{2\pi}\int_{-\infty}^{\infty} X(\Omega) e^{i\Omega t} \cdot e^{i(\Delta\alpha\cdot\Omega+\Delta\beta)} d\Omega , \quad \textbf{(3)}$$

After simplification, we can get:

$$x_n(t)=x(t+\Delta\alpha)e^{i\Delta\beta}. \quad (4)$$

This means that the carrier-envelope phase of the time domain signal changes by $\Delta\beta$ when the intercept of the phase spectrum changes $\Delta\beta$, as shown in Figs. 4(a) and 4(b) ($\Delta\alpha=0$ and $\Delta\beta=\pi/2$). When the slope of the phase spectrum changes by $\Delta\alpha$, the time domain signal shifts $\Delta\alpha$ in time, as shown in Figs. 4(c) and 4(d) ($\Delta\alpha=0.26$ ps and $\Delta\beta=0$). Therefore, modification of a THz waveform (including time shift and carrier-envelope phase change) could be contributed by the change of the slope ($\Delta\alpha$) and the intercept ($\Delta\beta$) in its phase spectrum.

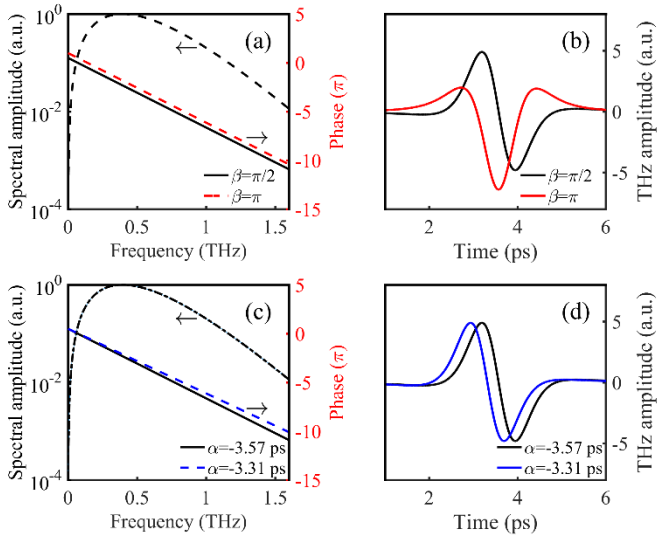

Fig. 4. (a) The amplitude spectrum (short dashed line) and two phase spectra with different intercepts ($\beta=\pi/2$ for solid line and $\beta=\pi$ for dashed line) when the slope of the phase spectra is -3.57 ps. Their corresponding THz waveforms are shown in (b). (c) The amplitude spectrum (dot dashed line) and two phase spectra with different slopes (α=-3.57 ps for solid line and $\alpha=-3.31$ ps for dashed line) when the intercept of the phase spectra is $\pi/2$. Their corresponding THz waveforms are shown in (d).

In our experiment, the measured THz signal in the far field [as Fig. 5(a)] is a coherent superposition of THz radiation emitted from different point sources along the filament, which is mainly contributed by THz radiation from plasma zone with a DC-bias. As this DC-bias is located at z, the phase of the emitted THz wave in the frequency domain can be written as:

$$\varphi=\varphi_0-\varphi_1(z)-\frac{\Omega}{c}l(z), \quad (5)$$

where c is the velocity of light, $l(z)$ is the propagation distance from the source to the detector in the far field. In Eq. (5), the first part, φ_0, is the initial carrier-envelope phase of the THz radiation, which keeps constant for any point source along the filament. The second part of Eq. (5), $\varphi_1(z)$, could be written as $\varphi_1(z)=\frac{\Omega}{c}z\frac{\upsilon^{800}}{\upsilon^{THz}}+\phi_G$, where υ^{THz} is the velocity of the THz pulse and υ^{800} is the velocity of the optical pump. The first term of $\varphi_1(z)$ comes from the velocity mismatch and the second term of $\varphi_1(z)$ comes from the

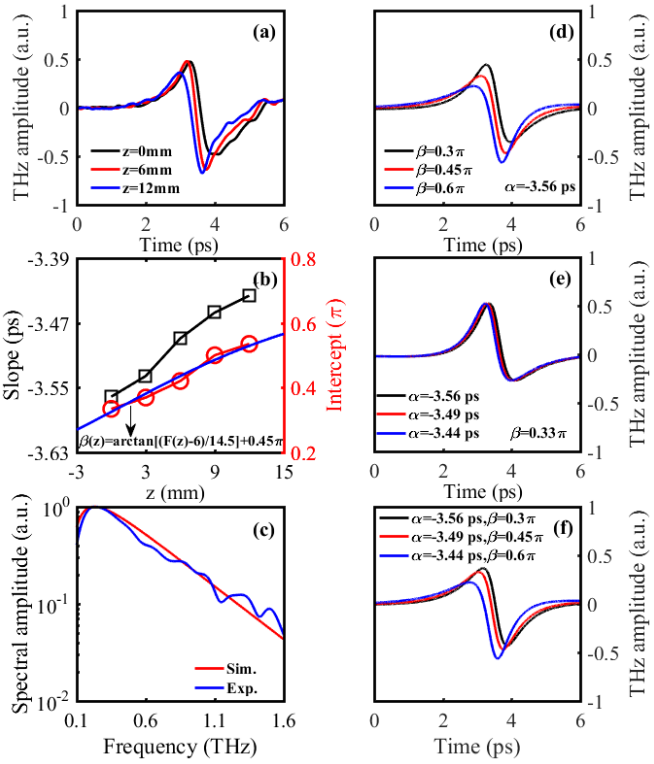

Fig. 5. (a) Measured THz waveform from air plasmas with slice-shaped DC-bias at z=0, 6, 12 mm. (b) The slope (black rectangles) and the intercept (red circles) of the THz phase spectrum versus different DC-bias positions. (c) Typical THz spectra, with the blue curve from measurement and red curve for simulation. The retrieved THz waveforms from simulation as a function of the intercept of the phase spectrum only (d), slope of the phase spectrum only (e), and both of the intercept and the slope of the phase spectrum (f), respectively.

contribution of the Gouy phase shift [20]. The velocity mismatch mainly affects the slope of the THz phase spectrum and the Gouy phase shift mainly affects the intercept of the THz phase spectrum. In case of $l(z)=0$, for example, when there is no velocity mismatch between the optical pump and the THz pulse, the slope of the phase spectrum will not change, i.e., no time shift of the THz pulse. When velocity mismatch between the optical pump and the THz pulse occurs, it results in an increase in the slope of the THz phase spectrum, i.e., a temporal advance of the THz pulse, as shown in Fig. 4(c) and Fig. 4(d). We can fit the experimental data as $\varphi=\alpha(z)\Omega+\beta(z)$. If $\alpha(z)$ and $\beta(z)$ are determined, however, it is still impossible to estimate the value of $\upsilon^{800}/\upsilon^{THz}$ due to the complexity of $l(z)$. Figure 5(b) shows the intercepts of the phase spectra (see red circles) of THz waves measured when the slice-shaped DC-bias is located at different positions. This tells that the intercept of the phase spectrum obeys the relation of the Gouy phase shift $\phi_G(z')=-\arctan(z'/z_R)$ when z' changes within a small range [21], z' is the distance from the THz focus to the EO crystal. Here z_R is the Rayleigh length of the THz pulse. In our case, the diameter of the THz beam irradiated on the off-axis parabolic mirror is D= 32.4mm and the focal length of the off-axis parabolic mirror is f= 100mm, the peak frequency of the THz wave is about 0.23 THz, one can estimate the THz beam waist after the parabolic mirror $w_0=2.5\,mm$ and the corresponding

Rayleigh length $z_R = 14.5\,mm$. With this, we can fit the intercept well with $\beta(z)=\varphi_0 + \arctan[\frac{F(z)-6}{z_R}]$ according to the Eq. (5) (see blue curve in Fig. 5(b)), where $F(z) = f - 1/[0.02 - 1/(z+f)]$ and $\varphi_0 = 0.45\,\pi$. And its influence on the waveform of the THz signal is shown in Fig. 5(d). The third part of Eq.(5), $\frac{\Omega}{c} l(z)$, is the phase variation due to the propagation effect of the THz wave when it propagates from the source to the detector in far field. It also affects the slope of the THz phase spectrum. The measured slopes of the THz phase spectra (black rectangles) versus the DC-bias position is shown in Fig. 5(b). Its corresponding effect on the THz waveform is shown in Fig. 5(e). When considering the velocity mismatch between the optical pump and the THz pulse, the THz propagation effect and the Gouy phase shift, we can retrieve the THz waveforms radiated from air plasmas with slice-shaped DC-bias at z=0, 6, 12 mm [Fig. 5(f)], which well agrees with the measured THz waveforms in Fig. 5(a).

The slope of the phase spectrum or the THz pulse delay is also related to the pump laser energy in addition to the DC-bias position. Figure 6 shows that the slopes of the THz phase spectrum increase when the laser energy increases. This suggests a temporal advance of the emitted THz pulse with an increase in laser energy. Therefore, higher laser energy creates a longer laser plasma filament, and thus leads to faster propagation of the emitted THz pulse, in agreement with our previous observation [17].

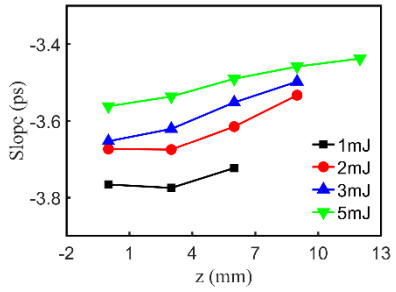

Fig. 6. Relationship between the slope of the THz phase spectrum and DC-bias position z for different laser energies.

In summary, we have investigated the phase evolution of THz waveforms from femtosecond laser-induced air plasma by controlling the DC-bias position along the filament. It is found that the variation of the THz waveforms is caused by the combined effects of the temporal shift of the THz waveform and the changes of the carrier-envelope phase of the THz pulse when the DC-bias position is moved. The slope of the phase spectrum determines the shift of the THz waveforms temporally and the intercept of the phase spectrum determines the changes of the carrier-envelope phases of the THz pulses. As the position of the applied DC-biased field moves to the beginning of the laser filament, the intercept of the phase spectrum or the carrier-envelope-phase changes, which is related to the Gouy phase shift. The velocity mismatch between the THz pulse and the optical pump, together with the THz propagation effect between the point source and the detector in far field, leads to an increase in the slope of the THz phase spectrum or a temporal shift of the THz pulse. These effects also exist when using a two-color laser scheme for THz radiation. In such case, the phase evolution of the THz pulse is dominated not only by combined effects mentioned above but also the phase difference between the two-color laser components. By clarifying the temporal order of the THz wave generation at different positions of the filament, the general understanding of the generation mechanism of the THz radiation from the femtosecond laser-induced air plasma can be enhanced.

Funding. The National Natural Science Foundation of China (Grant No. 11774228, 11655002, 11721091, 11474202 and 11991070) and Science and Technology Commission of Shanghai Municipality (Grant No. 16DZ2260200).

Disclosures: The authors declare no conflicts of interest.

REFERENCES

1. T. Bartel, P. Gaal, K. Reimann, M. Woerner, and T. Elsaesser, Opt. Lett **30**, 2805-2807 (2005).
2. N. Karpowicz, J. Dai, X. Lu, Y. Chen, M. Yamaguchi, H. Zhao, X.-C. Zhang, L. Zhang, C. Zhang, and M. Price-Gallagher, Appl. Phys. Lett **92**, 011131 (2008).
3. R. Ulbricht, E. Hendry, J. Shan, T. F. Heinz, and M. Bonn, Rev. Mod. Phys. **83**, 543 (2011).
4. M. C. Beard, G. M. Turner, and C. A. Schmuttenmaer, Phys. Rev. B **62**, 15764 (2000).
5. M. C. Hoffmann, J. Hebling, H. Y. Hwang, K.-L. Yeh, and K. A. Nelson, Phys. Rev. B **79**, 161201 (2009).
6. J. Dai, X. Xie, and X.-C. Zhang, Phys. Rev. Lett **97**, 103903 (2006).
7. K. Mori, M. Hashida, T. Nagashima, D. Li, K. Teramoto, Y. Nakamiya, S. Inoue, and S. Sakabe, AIP Advances **9**, 015134 (2019).
8. K.-Y. Kim, J. H. Glownia, A. J. Taylor, and G. Rodriguez, Opt. Express **15**, 4577-4584 (2007).
9. Y. Bai, L. Song, R. Xu, C. Li, P. Liu, Z. Zeng, Z. Zhang, H. Lu, R. Li, and Z. Xu, Phys. Rev. Lett **108**, 255004 (2012).
10. J. Zhao, Y. Zhang, Z. Wang, W. Chu, B. Zeng, W. Liu, Y. Cheng, and Z. Xu, Laser Phys. Lett **11**, 095302 (2014).
11. N. Li, Y. Bai, T. Miao, P. Liu, R. Li, and Z. Xu, Opt. Express **24**, 23009-23017 (2016).
12. X. Li, Y. Bai, N. Li, and P. Liu, Opt. Lett **43**, 114-117 (2018).
13. Z. Zhang, Y. Chen, M. Chen, Z. Zhang, J. Yu, Z. Sheng, and J. Zhang, Phys. Rev. Lett **117**, 243901 (2016).
14. T.-J. Wang, J. Ju, Y. Liu, R. Li, Z. Xu, and S. Leang Chin, Appl. Phys. Lett **110**, 221102 (2017).
15. N. Panov, O. Kosareva, V. Andreeva, A. Savel'ev, D. Uryupina, R. volkov, V. Makarov, A. Shkurinov, JETP Lett 93, 638(2011).
16. Y. You, T. Oh, and K. Kim, Phys. Rev. Lett **109**, 183902 (2012).
17. Z. Zhang, Y. Chen, S. Cui, F. He, M. Chen, Z. Zhang, J. Yu, L. Chen, Z. Sheng, and J. Zhang, Nature Photonics **12**, 554 (2018).
18. Y. Chen, T.-j. Wang, C. Marceau, F. Théberge, M. Châteauneuf, J. Dubois, O. Kosareva, and S. L. Chin, Appl. Phys. Lett. **95**, 101101 (2009).
19. J. R. Fienup, Opt. Lett **3**, 27-29 (1978).
20. S. Feng and H. G. Winful, Opt. Lett **26**, 485-487(2001).
21. A. B. Ruffin, J.V. Rudd, J.F. Whitaker, S. Feng, and H.G. Winful, Phys. Rev. Lett. **83**, 3410-3413(1999).

REFERENCES

1. T. Bartel, P. Gaal, K. Reimann, M. Woerner, and T. Elsaesser, "Generation of single-cycle THz transients with high electric-field amplitudes," Optics Letters **30**, 2805-2807 (2005).
2. N. Karpowicz, J. Dai, X. Lu, Y. Chen, M. Yamaguchi, H. Zhao, X.-C. Zhang, L. Zhang, C. Zhang, and M. Price-Gallagher, "Coherent heterodyne time-domain spectrometry covering the entire “terahertz gap”," Applied Physics Letters **92**, 011131 (2008).
3. R. Ulbricht, E. Hendry, J. Shan, T. F. Heinz, and M. Bonn, "Carrier dynamics in semiconductors studied with time-resolved terahertz spectroscopy," Reviews of Modern Physics **83**, 543 (2011).
4. M. C. Beard, G. M. Turner, and C. A. Schmuttenmaer, "Transient photoconductivity in GaAs as measured by time-resolved terahertz spectroscopy," Physical Review B **62**, 15764 (2000).
5. M. C. Hoffmann, J. Hebling, H. Y. Hwang, K.-L. Yeh, and K. A. Nelson, "Impact ionization in InSb probed by terahertz pump—terahertz probe spectroscopy," Physical Review B **79**, 161201 (2009).
6. J. Dai, X. Xie, and X.-C. Zhang, "Detection of broadband terahertz waves with a laser-induced plasma in gases," Physical Review Letters **97**, 103903 (2006).
7. K. Mori, M. Hashida, T. Nagashima, D. Li, K. Teramoto, Y. Nakamiya, S. Inoue, and S. Sakabe, "Increased energy of THz waves from a cluster plasma by optimizing laser pulse duration," AIP Advances **9**, 015134 (2019).
8. K.-Y. Kim, J. H. Glownia, A. J. Taylor, and G. Rodriguez, "Terahertz emission from ultrafast ionizing air in symmetry-broken laser fields," Optics Express **15**, 4577-4584 (2007).
9. Y. Bai, L. Song, R. Xu, C. Li, P. Liu, Z. Zeng, Z. Zhang, H. Lu, R. Li, and Z. Xu, "Waveform-controlled terahertz radiation from the air filament produced by few-cycle laser pulses," Physical Review Letters **108**, 255004 (2012).
10. J. Zhao, Y. Zhang, Z. Wang, W. Chu, B. Zeng, W. Liu, Y. Cheng, and Z. Xu, "Propagation of terahertz wave inside femtosecond laser filament in air," Laser Physics Letters **11**, 095302 (2014).
11. N. Li, Y. Bai, T. Miao, P. Liu, R. Li, and Z. Xu, "Revealing plasma oscillation in THz spectrum from laser plasma of molecular jet," Optics Express **24**, 23009-23017 (2016).
12. X. Li, Y. Bai, N. Li, and P. Liu, "Absorption of laser plasma in competition with oscillation currents for a terahertz spectrum," Optics Letters **43**, 114-117 (2018).
13. Z. Zhang, Y. Chen, M. Chen, Z. Zhang, J. Yu, Z. Sheng, and J. Zhang, "Controllable terahertz radiation from a linear-dipole array formed by a two-color laser filament in air," Physical Review Letters **117**, 243901 (2016).
14. T.-J. Wang, J. Ju, Y. Liu, R. Li, Z. Xu, and S. Leang Chin, "Waveform control of enhanced THz radiation from femtosecond laser filament in air," Applied Physics Letters **110**, 221102 (2017).
15. N. Panov, O. Kosareva, V. Andreeva, A. Savel’ev, D. Uryupina, R. volkov, V. Makarov, A. Shkurinov, JETP Letters 93, 638(2011).
16. Y. You, T. Oh, and K. Kim, "Off-axis phase-matched terahertz emission from two-color laser-induced plasma filaments," Physical Review Letters 109, 183902 (2012).
17. Z. Zhang, Y. Chen, S. Cui, F. He, M. Chen, Z. Zhang, J. Yu, L. Chen, Z. Sheng, and J. Zhang, "Manipulation of polarizations for broadband terahertz waves emitted from laser plasma filaments," Nature Photonics **12**, 554 (2018).
18. Y. Chen, T.-j. Wang, C. Marceau, F. Théberge, M. Châteauneuf, J. Dubois, O. Kosareva, and S. L. Chin, "Characterization of terahertz emission from a dc-biased filament in air," Applied Physics Letters **95**, 101101 (2009).
19. J. R. Fienup, "Reconstruction of an object from the modulus of its Fourier transform," Optics Letters **3**, 27-29 (1978).
20. S. Feng and H. G. Winful, "Physical origin of the Gouy phase shift", Optics Letters **26**, 485-487(2001).
21. A. B. Ruffin, J.V. Rudd, J.F. Whitaker, S. Feng, and H.G. Winful, "Direct observation of the Gouy phase shift with single-cycle terahertz pulses",Physics Review Letters **83**, 3410-3413(1999).